MD, PhD, on the influence of the transient equilibrium of [^{123}I]-FPCIT on the striatal V_3'' values in healthy subjects. The authors also acknowledge the nuclear medicine technologist support of Michele Early, Eileen Smith and Gary Wisniewski; data analysis by Michele Early; clinical coordination and support by Barbara Fussell and the radiochemistry technical help of Yolanda Zea-Ponce, PhD, and Morgan Stratton.

REFERENCES

1. Neumeyer JL, Wang S, Milius RA, et al. Iodine-123-2- β-Carbomethoxy-3-β-(4-iodophenyl)-tropane ([^{123}I]β-CIT): high affinity SPECT radiotracer of monoamine reuptake sites in brain. *J Med Chem* 1991;34:3144–3146.
2. Innis R, Seibyl J, Scanley B, et al. SPECT imaging demonstrates loss of striatal monoamine transporters in Parkinson's disease. *Proc Natl Acad Sci USA* 1993;90: 11965–11969.
3. Laruelle M, Baldwin R, Malison R, et al. SPECT imaging of dopamine and serotonin transporters with [^{123}I]β-CIT: pharmacological characterization of brain uptake in nonhuman primates. *Synapse* 1993;13:295–309.
4. Seibyl J, Wallace E, Smith E, et al. Whole-body biodistribution, radiation absorbed dose and brain SPECT imaging with [^{123}I]β-CIT in healthy human subjects. *J Nucl Med* 1994;35:764–770.
5. Laruelle M, Wallace E, Seibyl J, et al. Graphical, kinetic and equilibrium analyses of in vivo [^{123}I]β-CIT binding to dopamine transporters in healthy human subjects. *J Cereb Blood Flow Metab* 1994;14:982–994.
6. van Dyck C, Seibyl J, Malison R, et al. Age-related decline in striatal dopamine transporter binding with iodine-^{123}I-β-CIT SPECT. *J Nucl Med* 1995;36:1175–1181.
7. Seibyl J, Marek K, Quinlan D, et al. Decreased SPECT [^{123}I]β-CIT striatal uptake correlates with symptom severity in Parkinson's disease. *Ann Neurol* 1995;38:589–598.
8. Rinne J, Kuikka J, Bergstrom K, Rinne U. Striatal dopamine transporter in different disability stages of Parkinson's disease studied with [123-I]-β-CIT SPECT. *Parkinsonism Rel Disord* 1995;1:47–51.
9. Brucke T, Kornhuber J, Angelberger P, Asenbaum S, Frassine H, Podreka I. SPECT imaging of dopamine and serotonin transporters with [^{123}I]β-CIT binding kinetics in the human brain. *J Neural Transm Gen Sect* 1993;94:137–146.
10. Asenbaum S, Brucke T, Pirker W, et al. Imaging of dopamine transporters with iodine-123-β-CIT and SPECT in Parkinson's disease. *J Nucl Med* 1997;38:1–6.
11. Marek K Seibyl J, Zoghbi S, et al. Iodine-123 β-CIT SPECT imaging demonstrates bilateral loss of dopamine transporters in hemi-parkinson's disease. *Neurology* 1996;46:231–237.
12. Seibyl J, Laruelle M, van Dyck C, et al. Reproducibility of [^{123}I]-β-CIT SPECT brain measurement of dopamine transporters in healthy human subjects. *J Nucl Med* 1996;37:222–228.
13. Baldwin R, Zea-Ponce Y, Zoghbi S, et al. Evaluation of the monoamine uptake site ligand [^{123}I]methyl 3β-(4-iodophenyl)-tropane-2?-carboxylate (^{123}I)β-CIT in nonhuman primates: pharmacokinetics, biodistribution and SPECT brain imaging coregistered with MRI. *Nucl Med Biol* 1993;20:597–606.
14. Abi-Dargham A, Gandelman MS, Erausquin G, et al. SPECT imaging of dopamine transporters in human brain with iodine-123-fluoroalkyl analogs of [^{123}I]-β-CIT. *J Nucl Med* 1996;37:1129–1133.
15. Booij J, Tissingh G, Winogrodzka A, et al. Practical benefit of [^{123}I]-FPCIT SPECT in the demonstration of the dopaminergic deficit in Parkinson's disease. *Eur J Nucl Med* 1997;24:68–71.
16. Kuikka J, Bergstrom K, Ahonen A, et al. Comparison of iodine-123 labeled 2β-carbomethoxy-3β-(4-iodophenyl)tropane and 2β-carbomethoxy-3β-(4-iodophenyl)-N-(3-flouropropyl)nortropane for imaging of the dopamine transporter in the living human brain. *Eur J Nucl Med* 1996;22:356–360.
17. Fahn S, Elton R, and members of the UPDRS development committee Unified Parkinson's disease rating scale. In: Fahn S, Marsden, CD, Calne, DB, Goldstein, M, eds. *Recent developments in Parkinson's disease*. Florham Park, NJ: Macmillan Healthcare Information; 1987:153–164.
18. Chang LT. A method for attenuation correction in computed tomography. *IEEE Trans Nucl Sci* 1987;NS-25:638–643.
19. Logan J, Fowler J, Volkow N, et al. Graphical analysis of reversible radioligand binding from time-activity measurements applied to [N-^{11}C-methyl]-(-)cocaine PET studies in human subjects *J Cereb Blood Flow Metab* 1990;10:740–747.
20. Gandelman M, Baldwin RM, Zoghbi SS, Zea-Ponce Y, Innis RB. Evaluation of ultrafiltration for the free fraction determination of SPECT radiotracers: β-CIT, IBF, and iomazenil. *J Pharm Sci* 1994;83:1014–1019.
21. Pirker W, Asenbaum S, Kasper S, et al. β-CIT SPECT demonstrates blockade of 5HT-uptake sites by citalopram in the human brain in vivo. *J Neural Transm* 1995;100:247–256.
22. Chinaglia G, Landwehrmeyer B, Probst A, Palacios JM. Serotoninergic terminal transporters are differentially affected in Parkinson's disease and progressive supranuclear palsy: an autoradiographic study with [^{3}H]citalopram. *Neuroscience* 1993;54: 691–699.
23. Bergstrom K, Halldin C, Kuikka J, et al. Lipophilic metabolite of [^{123}I]-β-CIT in human plasma may obstruct quantitation of the dopamine transporter. *Synapse* 1995;19:297–300.
24. Bergstrom KA, Halldin C, Kuikka JT, et al. The metabolite pattern of [^{123}I]-β-CIT determined with a gradient HPLC method. *Nucl Med Biol* 1995;22:971–976.
25. Bergstrom KA, Halldin C, Lundkvist C, et al. Characterization of ^{11}C or ^{123}I labeled β-FPCITand β-CIT-FE metabolism measured in monkey and human plasma—identification of two labeled metabolites with HPLC. *Hum Psychopharm* 1996;11: 483–490.
25. Coenen H, Dutschka K, Muller S, et al. NCA radiosynthesis of [^{123,124}I]-β-CIT, plasma analysis and pharmacokinetic studies with SPECT and PET. *Nucl Med Biol* 1995;22:977–984.
27. Iwasaki Y, Yonekura Y, Saji H, et al. SPECT imaging of dopamine D2 receptors with 2' iodospiperone. *J Nucl Med* 1995;36:1191–1195.
28. Swahn C-G, Halldin C, Bergstrom K, Lundkvist C, Farde L. Carbon-11 and ^{123}I labeled 2β carbomethoxy-3β-(4-iodophenyl)tropane (β-CIT) derivatives and their labeled metabolites in monkey and human plasma determined by gradient HPLC. *J Label Comp Radiopharm* 1995;37:706–708.
29. Heinz A, Jones DW, Gorey JG, et al. Analysis of the metabolites of [^{123}I-]-β-CIT in plasma of human and nonhuman primates. *Synapse* 1997;25:306–308.
30. Carson R, Channing M, Blasberg R, et al. Comparison of bolus and infusion methods for receptor quantitation:application to [^{18}F]cyclofoxy and positron emission tomography. *J Cereb Blood Flow Metab* 1993;13:24–42.
31. Farde L, Eriksson L, Blomquist G, Halldin C. Kinetic analysis of central [^{11}C] raclopride binding to D2 dopamine receptors studies with PET—a comparison to the equilibrium analysis. *J Cereb Blood Flow Metab* 1989;9:696–708.

Discordance of Technetium-99m-HMPAO and Technetium-99m-ECD SPECT in Herpes Simplex Encephalitis

Harald Rieck, Cornelia Adelwöhrer, Karin Lungenschmid and Eberhard Deisenhammer
Departments of Neurology and Neuroradiology, Landesnervenklinik Linz, Linz, Austria

Technetium-99m-hexamethyl propyleneamine oxime (HMPAO) and ^{99m}Tc-ethyl cysteinate dimer (ECD) accumulate in brain tissue in proportion to regional cerebral blood flow in healthy subjects and in patients with a variety of neurological diseases. We report on four patients with herpes simplex encephalitis and the discordance between these two approved cerebral perfusion imaging radiopharmaceuticals. **Conclusion:** SPECT images showed unilateral regional increase of ^{99m}Tc-HMPAO uptake and decrease of ^{99m}Tc-ECD uptake in the affected temporal lobe.

Key Words: SPECT; technetium-99m-hexamethyl propyleneamine oxime; technetium-99m-ethyl cysteinate dimer; herpes simplex encephalitis

J Nucl Med 1998; 39:1508–1510

Received Jul. 21, 1997; revision accepted Dec. 19, 1997.
For correspondence or reprints contact: Harald Rieck, MD, Landesnervenklinik Linz, Wagner Jauregg-Weg 15, A-4020 Linz, Austria.

After intravenous administration, ^{99m}Tc-hexamethyl propyleneamine oxime (HMPAO; Ceretec; Amersham, United Kingdom) and N,N'−1,2-ethylene-diylbis-L-cysteine diethyl ester (ECD;

TABLE 1
Clinical Signs and Laboratory Findings

Findings	Patient 1	2	3	4
Age (yr)	62	62	46	58
Sex	F	F	F	M
Clinical signs				
Fever	X	X	X	X
Headache	X	X		X
Nuchal rigidity		X	X	X
Somnolence	X	X		X
Confusion		X	X	
Disorientation			X	
Memory disorders		X	X	X
Vertigo, nausea	X	X		
Seizures	X		X	
Laboratory findings				
Cells/mm^3	150	27	912	277
Lymphocytes/mm^3	135	ND	752	272
Protein (mg/dl)	47	38	68	78
Serology				
HSV-IgM (liqu)	−	+	ND	−
HSV-IgG (liqu)	+	+++	ND	+
HSV-I PCR (liqu)	ND	ND	+	−

HSV = herpes simplex virus; ND = not done; PCR = polymerase chain reaction; + = positive; − = negative; +++ = very high positive.

Neurolite; DuPont Merck, Bad Homburg, Germany) accumulate in normal brain tissue according to the regional cerebral blood flow (rCBF).

Xenon-133 is the most well-established tracer used to study quantitative rCBF. Therefore, it was used to determine the ability of HMPAO and ECD to follow rCBF (*1,2*). Comparison of HMPAO and ECD with ^{133}Xe showed similar distribution patterns in healthy subjects and under a variety of pathological conditions (*1–10*).

In herpes simplex encephalitis (HSE), Launes et al. (*11*) reported an increased uptake of ^{99m}Tc-HMPAO in the affected temporal lobes, which has been confirmed by other investigators (*12–18*). We present a series of HSE patients with an unexpected discrepancy between HMPAO and ECD SPECT findings.

MATERIALS AND METHODS

We investigated clinical, MRI and HMPAO and ECD SPECT features in four adult patients with HSE. The clinical symptoms and laboratory findings are shown in Table 1. All patients responded to acyclovir treatment, with resolution of acute symptoms within a few days.

The initial ^{99m}Tc-HMPAO and ^{99m}Tc-ECD SPECT and MRI were performed within 4 wk after clinical onset. We then repeated the HMPAO SPECT to confirm previous findings. The time sequence of the investigations is summarized in Table 2.

TABLE 2
Time Delay in Days from Clinical Onset to SPECT and MRI Studies

Patient no.	HMPAO 1	ECD	HMPAO 2	MRI
1	8	22	25	9, 25
2	27	31	50	28, 50
3	9	11	21	10, 21
4	21	24	27	14

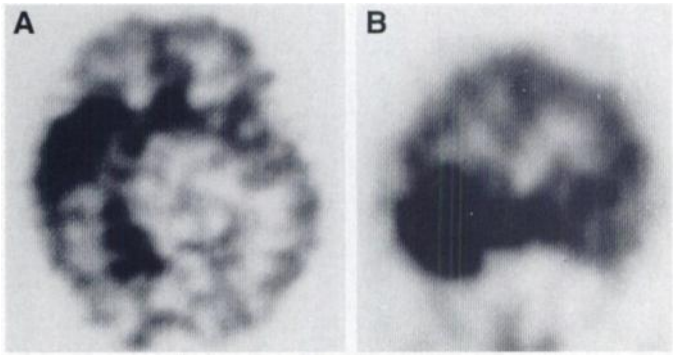

FIGURE 1. SPECT images of Patient 2. Axial slices parallel to and 24 mm above the canthomeatal line (A) and coronal slices (B) are shown. Note increased uptake of ^{99m}Tc-HMPAO in right temporal lobe.

SPECT Procedure

Tracer labeling was performed according to the manufacturers' instructions. After intravenous injection of 20 mCi HMPAO and ECD, data acquisition was initiated within 20 min and 60 min, respectively, on a three-head, rotating gamma camera (Prism 3000; Picker International, Cleveland, OH) with high-resolution, low-energy collimators. The rotation time was 20 min, and 120 projections were acquired in steps of 3°. The raw data were processed by special software (Mirage; Mirage Imaging Processing Systems Ltd., Vienna, Austria) using prereconstruction scatter and attenuation correction (*19*). After reorientation along the canthomeatal line, axial, coronal and sagittal 3-mm slices were obtained for visual analysis.

RESULTS

SPECT images showed increased uptake of ^{99m}Tc-HMPAO in the affected temporal lobes in all four patients. Additional involvement of the adjacent paramedian structures was seen in Patients 2 and 3 (Fig. 1). This phenomenon was still present in the second control investigation after clinical recovery. However, ^{99m}Tc-ECD uptake was clearly decreased in the same areas (Fig. 2).

SPECT findings were well congruent with signal alterations in MRI (Fig. 3). Initial gadolinium-diethylenetriamine pentaacetic acid enhancement was observed in only Patients 2 and 4.

DISCUSSION

We found increased uptake of ^{99m}Tc-HMPAO in the affected temporal lobe and adjacent brain structures in acute HSE. This observation has also been reported in HSE by other investigators (*11–18*), but has not been observed in nonherpetic encephalitis. Most authors interpreted this finding as the consequence

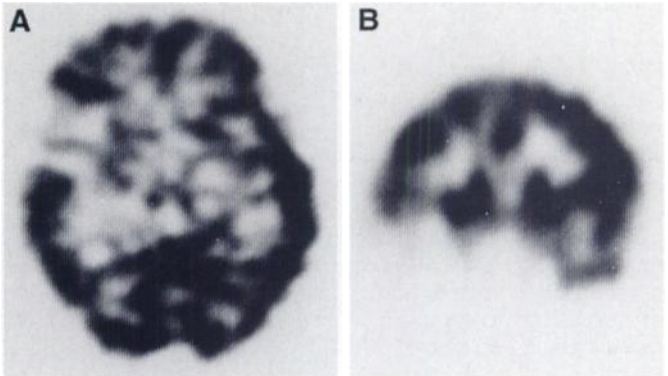

FIGURE 2. SPECT images of Patient 2. Note decreased uptake of ^{99m}Tc-ECD in right temporal lobe. Compare with uptake of ^{99m}Tc-HMPAO in Figure 1.

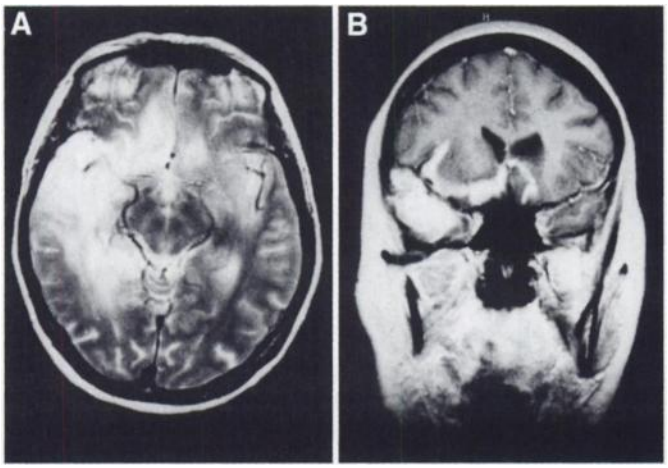

FIGURE 3. T2-weighted MR images of Patient 2. Signal hyperintensity in right temporal lobe is congruent with increased uptake of ^{99m}Tc-HMPAO and decreased uptake of ^{99m}Tc-ECD (Figs. 1 and 2, respectively).

of hyperperfusion, whereas others attributed it to additional metabolic trapping mechanisms of HMPAO (*11,16*).

Technetium-99m-HMPAO uptake correlated well with normal and decreased (*1,2*) but not very high rCBF values in abnormal brain tissue. In subacute ischemic stroke, exaggerated uptake of ^{99m}Tc-HMPAO exceeded the real perfusion measured by ^{133}Xe-SPECT (*20*). In contrast, ^{99m}Tc-ECD did not show hyperemia in subacute stroke (*21*).

Uptake of ECD was reduced in corresponding areas of increased HMPAO uptake in HSE. This was not due to the time course of the underlying brain pathology, as demonstrated by repeat HMPAO SPECT.

In our opinion, uptake of both blood flow tracers does not reflect only perfusion in HSE. Disturbed membrane and intracellular metabolism (*11,16,22*) may also change tracer kinetics and lead to discordant uptake of both agents.

CONCLUSION

Under certain pathological conditions, the uptake of both brain perfusion radiopharmaceuticals may be influenced by altered cell metabolism or membrane characteristics at the blood-brain barrier. Therefore, careful consideration of the underlying pathology is indispensable for interpretation of SPECT results as hyper- or hypoperfusion.

REFERENCES

1. Payne JK, Madhukar HT, Devous MD. Comparison of technetium-99m-HMPAO and xenon-133 measurements of regional cerebral blood flow by SPECT. *J Nucl Med* 1996;37:1735–1740.
2. Devous MD, Payne JK, Lowe JL, Leroy RF. Comparison of technetium-99m-ECD to xenon-133 SPECT in normal controls and in patients with mild to moderate regional cerebral blood flow abnormalities. *J Nucl Med* 1993;34:754–761.
3. Murase K, Tanada S, Fujita H, Sakaki S, Hamamoto K. Kinetic behavior of technetium-99m-HMPAO in the human brain and quantification of cerebral blood flow using dynamic SPECT. *J Nucl Med* 1992;33:135–143.
4. Friberg L, Andersen AR, Lassen NA, Holm S, Dam M. Retention of ^{99m}Tc-bicisate in the human brain after intracarotid injection. *J Cereb Blood Flow Metab* 1994;14(suppl 1):S19–S27.
5. Greenberg JH, Lassen NA. Characterization of ^{99m}Tc-bicisate as an agent for the measurement of cerebral blood flow with SPECT. *J Cereb Blood Flow Metab* 1994;14(suppl 1):S1–S3.
6. Leveille J, Demonceau G, Walovitch RC. Intrasubject comparison between technetium-99m-ECD and technetium-99m-HMPAO in healthy human subjects. *J Nucl Med* 1992;33:480–484.
7. Pupi A, Castagnoli A, De Cristofaro MTR, Bacciottini L, Petti AR. Quantitative comparison between ^{99m}Tc-HMPAO and ^{99m}Tc-ECD: measurement of arterial input and brain retention. *Eur J Nucl Med* 1994;21:124–130.
8. Tsuchida T, Nishizawa S, Yonekura Y, et al. SPECT images of technetium-99m-ethyl cysteinate dimer in cerebrovascular diseases: comparison with other cerebral perfusion tracers and PET. *J Nucl Med* 1994;35:27–31.
9. Vallabhajosula S, Zimmerman RE, Picard M, et al. Technetium-99m ECD: a new brain imaging agent. In vivo kinetics and biodistribution studies in normal human subjects. *J Nucl Med* 1989;30:599–604.
10. Walovitch RC, Cheesman EH, Maheu LJ, Hall KM. Studies of the retention mechanism of the brain perfusion imaging agent ^{99m}Tc-bicisate (^{99m}Tc-ECD). *J Cereb Blood Flow Metab* 1994;14(suppl 1):S4–S11.
11. Launes J, Lindroth L, Liewendahl K, Nikkinen P, Brownell AL, Iivanainen M. Diagnosis of acute herpes simplex encephalitis by brain perfusion single photon emission computed tomography. *Lancet* 1988;1:1188–1191.
12. Duncan R, Patterson J, Bone I, Kennedy PGE. Single photon emission computed tomography in diagnosis of herpes simplex encephalitis. *Lancet* 1988;2:516.
13. Nara T, Nozaki H, Nishimoto H. Single photon emission computed tomography in diagnosis of herpes simplex encephalitis. *Lancet* 1988;2:516.
14. Nara T, Nozaki H, Nishimoto H. Brain perfusion in acute encephalitis: relationship to prognosis studied using SPECT. *Pediatr Neurol* 1990;6:422–424.
15. Lane R, Kirkbride V, Hughes P, Jones B, Costa D. Diagnosis of herpes simplex encephalitis by single photon emission tomography. *Lancet* 1989;1:778–779.
16. Schmidbauer M, Podreka I, Wimberger D, et al. SPECT and MR imaging in herpes simplex encephalitis. *J Comput Assist Tomogr* 1991;15:811–815.
17. Kao CH, Wang SJ, Mak SC, Shian WJ, Chi CS. Viral encephalitis in children: detection with technetium-99m HMPAO brain single-photon emission CT and its value in prediction of outcome. *Am J Neuroradiol* 1994;15:1369–1373.
18. Masdeu JC, Van Heertum RL, Abdel-Dayem H. Viral infections of the brain. *J Neuroimaging* 1995;5(suppl 1):S40–S44.
19. Bellini SM, Piacentini M, Cafforio C, Rocca F. Compensation of tissue absorption in emission tomography. *IEEE Trans Acous Speech Sign Proc ASSP* 1997;27:213–218.
20. Sperling B, Lassen NA. Hyperfixation of HMPAO in subacute ischemic stroke leading to spuriously high estimates of cerebral blood flow in SPECT. *Stroke* 1993;24:193–194.
21. Lassen NA, Sperling B. ^{99m}Tc-bicisate reliably images CBF in chronic brain diseases but fails to show reflow hyperemia in subacute stroke: report of a multicenter trial of 105 cases comparing ^{133}Xe and ^{99m}Tc-bicisate (ECD, Neurolite) measured by SPECT on same day. *J Cereb Blood Flow Metab* 1994;14(suppl 1):S44–S48.
22. Jacquier-Sarlin MR, Polla BS, Slosman DO. Oxido-reductive state: the major determinant for cellular retention of technetium-99m-HMPAO. *J Nucl Med* 1996;37:1413–1416.